Relationships between local order and magnetic behavior in amorphous $Fe_{0.30}Y_{0.70}$: Extended x-ray-absorption fine structure and susceptibility

T. I. Morrison,* C. L. Foiles, D. M. Pease, and N. J. Zaluzec

Materials Science Division, Argonne National Laboratory, Argonne, Illinois 60439

(Received 26 September 1986)

X-ray-absorption near-edge-structure spectroscopy, extended x-ray-absorption fine-structure spectroscopy, electron energy-loss spectroscopy, and susceptibility measurements have been used to study the relationships between local order, d-band occupancy, and magnetic properties in amorphous $Fe_{0.30}Y_{0.70}$. All the results can be interpreted as being due to the existence of amorphous iron clusters in an amorphous yttrium matrix. The relations between structure and magnetic properties in amorphous binary alloys are discussed.

I. INTRODUCTION

Magnetism in amorphous alloys has been the subject of intense discussion and study for two decades. A great deal of work has appeared in the literature in this field in general and on amorphous iron-yttrium alloys in particular,[1] indicating the high degree of fundamental interest and technological importance of these alloys. Progress has been hampered, though, by a lack of detailed structural information in noncrystalline systems.

In order to completely understand the magnetic properties of amorphous alloys it is of crucial importance to know in detail the short-range order about the magnetic species. Recent extended x-ray-absorption fine structure (EXAFS) studies[2-4] have repeatedly demonstrated the inadequacy of a dense random packing of hard-spheres model; the possibility of clustering, or chemical short-range order (CSRO) must be taken into account since deviations from random packing will affect the electronic structure and magnetic behavior of the material. It is thus necessary to describe the environment of the magnetic atoms before explaining the bulk magnetic properties.

In order to more completely characterize the amorphous $Fe_{0.30}Y_{0.70}$ alloy, we have performed x-ray appearance rear-edge structure (XANES), EXAFS, electron-energy-loss spectroscopy (EELS), and magnetic-susceptibility measurements on triode sputtered samples. Together, EXAFS and XANES can describe the local environment of the atomic species,[2] EELS can measure changes in d-band occupancy,[5] and superconducting quantum-interference device (SQUID) susceptometry measurements can give the bulk magnetic behavior of the material. By combining these techniques we can arrive at a model consistent with the results of each and examine the relationships between structure and magnetic behavior in amorphous binary alloys.

II. EXPERIMENTAL PROCEDURE

Samples for XANES, EXAFS, and susceptibility measurements were prepared by argon-ion triode sputtering onto glass slides (EXAFS and XANES) and coverslips (susceptibility) from a $Fe_{0.35}Y_{0.65}$ (eutectic composition) target to thicknesses of 5000 Å. Samples for EELS mea-

surements were prepared by sputtering onto air-cleaved rock salt to a thickness of 300 Å. After deposition the EELS samples were floated off the rock salt in deionized water and mounted onto transmission-electron-microscope grids. The thicker samples showed no x-ray diffraction peaks, and the EELS samples were checked by transmission electron diffraction and showed only broad, diffuse scattering rings. The alloy composition was determined to be 30($\pm$5) at. % Fe and 70($\pm$5) at. % Y by electron-induced x-ray fluorescence.

XANES and EXAFS measurements on the amorphous alloy and on the intermetallic compound YFe_2 were made on the X-11A beamline at the National Synchrotron Light Source. Measurements on the amorphous alloy were made in fluorescence mode and on the intermetallic in transmission mode. All measurements were made at room temperature. In each case, the incident and transmitted or fluorescent intensities of several consecutive scans were summed to improve the signal-to-noise ratio. The iron K-edge XANES spectra for pure iron, crystalline YFe_2, and the amorphous $Fe_{0.30}Y_{0.70}$ alloy are shown in Fig. 1. The k-weighted iron and yttrium EXAFS spectra for the intermetallic and the amorphous alloy, normalized by procedures described elsewhere,[6] are shown in Fig. 2.

EELS spectra were made at the Argonne National Laboratory Electron Microscopy Center using a Phillips 420 transmission electron microscope operating at 120 kV. The energy-loss spectra were measured on a Gatan 607 energy-loss spectrometer. The energy resolution was less than 2 eV, and the 3.5-mrad acceptance angle assured the validity of the dipole approximation. The 300-Å thickness of the sample was chosen to minimize multiple-scattering events while maintaining the mechanical stability of the sample.

The magnetic measurements were done with an automated SQUID magnetometer. Portions of the amorphous $Fe_{0.30}Y_{0.70}$ film on its substrate were mounted with the applied field parallel to the film, and data were obtained for a number of field-temperature sequences. Portions of the substrate were subsequently measured using the same procedures and these data were used to identify the results associated with the amorphous alloy film. The weakest signal was 50 times greater than the detection
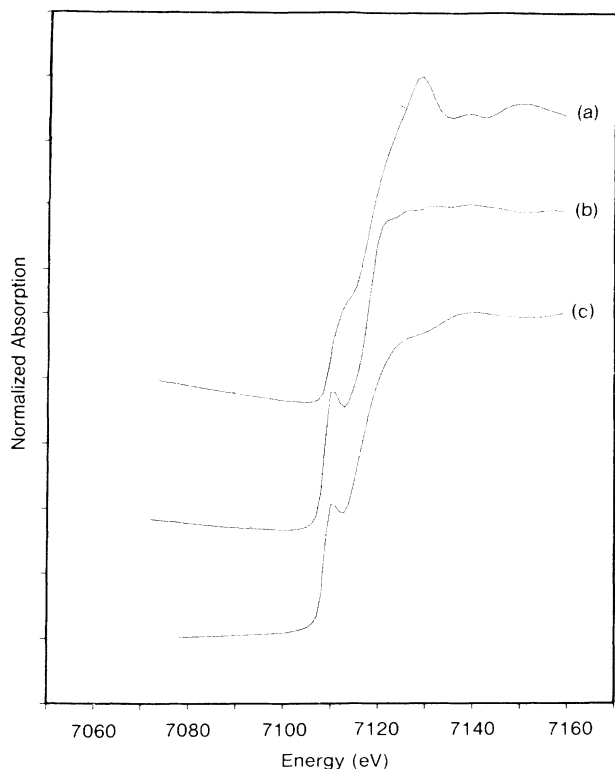
FIG. 1. Iron K-edge XANES for (a) pure Fe, (b) crystalline Fe_2Y, and (c) amorphous $Fe_{0.30}Y_{0.70}$.

limits of the system and the reproducibility checks indicate that 5% is an upper limit of error. All samples were mounted in a Kel-F bucket, whose magnetic properties were known and reverified, and the calibration of the magnetometer was verified using a NBS Pt standard.

III. RESULTS

A. EXAFS and XANES

The iron K-edge XANES data in Fig. 1 show significant differences between the bcc iron and the close-packed crystalline Fe_2Y. The differences in edge structure can be interpreted as reflecting the different packing arrangements,[7] and consequently the similarities between the Fe_2Y and the $Fe_{0.30}Y_{0.70}$ spectra indicate that both are nearly close packed; i.e., the iron atoms have 12 near neighbors in the amorphous alloy.

The EXAFS spectra shown in Fig. 2 immediately reveal a number of important points. First, it is apparent that even though the iron in the amorphous alloy is 12-coordinate, the Fe EXAFS amplitude of the alloy is much lower than in the intermetallic compound. In addition, the amplitude of the yttrium EXAFS of the alloy is smaller than even the amplitude of the iron EXAFS. It has been shown[8] that increases in disorder will greatly decrease EXAFS amplitudes, so it can be qualitatively inferred that the local environment of the yttrium is far more disordered than that of the iron.
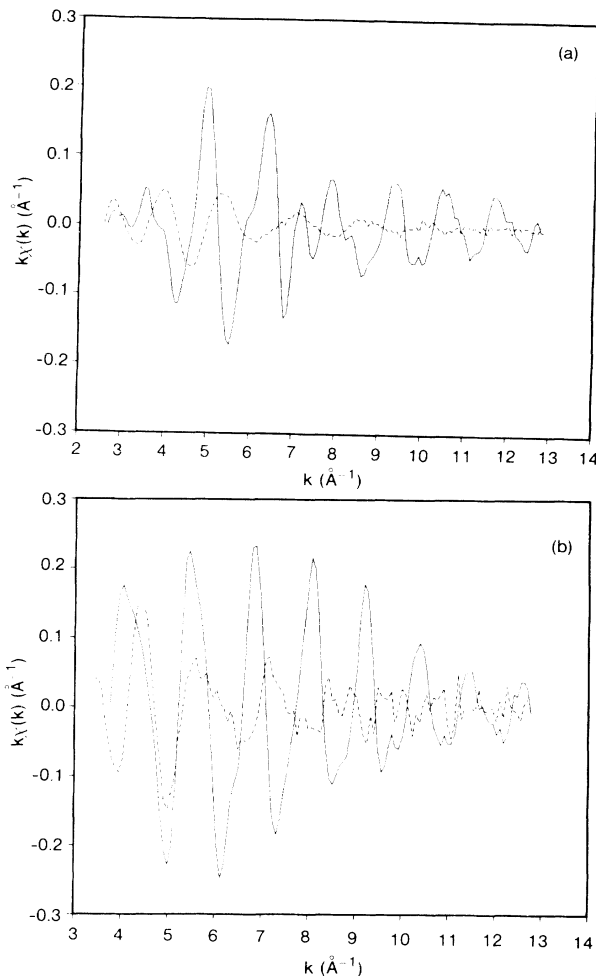

FIG. 2. (a) k-weighted iron and (b) yttrium K-edge EXAFS spectra of crystalline Fe_2Y (solid lines) and amorphous $Fe_{0.30}Y_{0.70}$ (dashed lines). Amplitude of the yttrium EXAFS in the amorphous alloy is multiplied by 10.

The absolute values of the Fourier transforms of the EXAFS, shown in Figs. 3(a) and 3(b), are useful in further interpreting the EXAFS data. In Fig. 3(a) it can be seen that there are only first-near-neighbor peaks in the Fourier transform of the iron EXAFS of the alloy, indicating complete amorphicity since peaks from more distant neighbors are absent. The Fourier transform of the yttrium EXAFS of the alloy shows only a weak structure near $R = 2.1$ Å. This structure is so small that it is comparable to the noise level and cannot be further analyzed with any degree of reliability.

By using a backtransform curve-fitting method described in Ref. 2, it is possible to deduce the local environment about the Fe atoms. We start by assuming model distribution functions[9] for Fe-Fe, Fe-Y, and Y-Y pairs:

$$g_j(r) = \begin{cases} (1/2\sigma_j^3)(r_j - r_{0j})\exp[-(r_j - r_{0j})/\sigma_j] , & r_j \geq r_{0j} \\ 0 , & r_j < r_{0j} \end{cases} \quad (1)$$

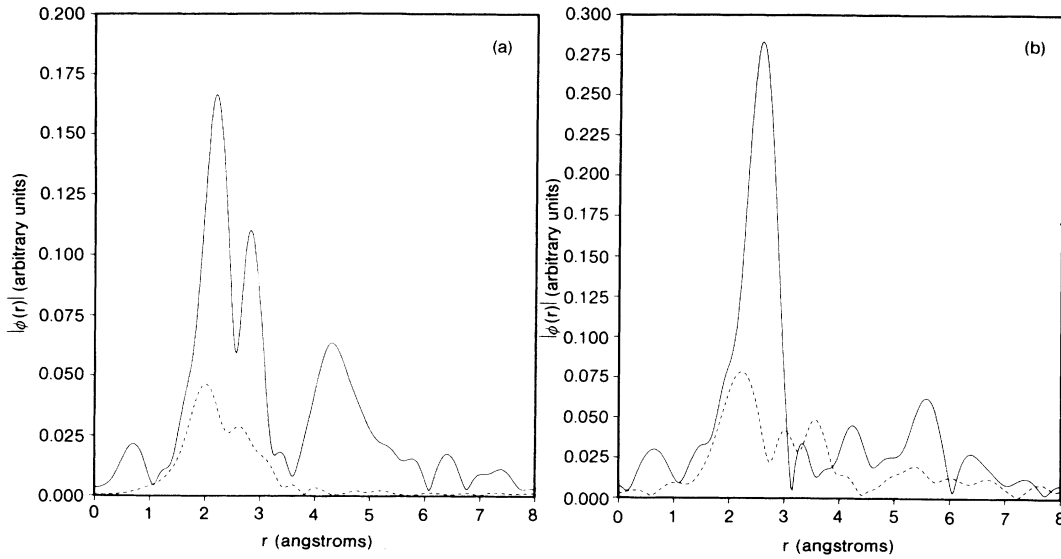where σ describes the disorder and asymmetry of the

FIG. 3. Amplitude of the Fourier transforms of (a) iron and (b) yttrium K-edge EXAFS spectra of crystalline Fe_2Y (solid lines) and amorphous $Fe_{0.30}Y_{0.70}$ (dashed lines). Amplitude of the transform of the yttrium EXAFS of the alloy is multiplied by 10.

$g_j(r)$ and r_{0j} is the closest approach of the atoms. This model, initially used to describe the EXAFS of liquids, is especially attractive in that it lets us write the EXAFS equation in a closed form:

$$\chi(k)=\sum_j \frac{N_j\,|\,f_j(\pi,k\,)\,|}{kr_{0j}^2}\;\frac{1}{1+(2k\sigma_j)^{3/2}}\sin$$

$$\times\left[2kr_{0j}+\alpha(k)+\tan^{-1}\right.$$

$$\left.\times\left[(2k\sigma_j)\frac{3-(2k\sigma_j)^2}{1-3(2k\sigma_j)^2}\right]\right],\qquad (2)$$

$$k=\left[\frac{2m_e}{\hbar^2}(h\nu-E_0)\right]^{1/2},\qquad (3)$$

where j denotes the jth backscattering shell, N_j is the number of atoms in the jth shell, $|\,f_j(\pi,k\,)\,|$ is the backscattering amplitude of the atoms in the jth shell, and $\alpha(k)$ is an absorber-backscatterer–dependent phase shift. E_0 is the photoejection threshold of the EXAFS event and $h\nu$ is the incident x-ray energy. It is possible to fit Eq. (2) to the backtransformed EXAFS data by varying the parameters N, R, σ, and E_0. In principle, it is desirable to fit the EXAFS spectra of both constituent atoms simultaneously, constraining $R_{A-B}=R_{B-A}$ and $\sigma_{A-B}=\sigma_{B-A}$. Such a simultaneous fitting was attempted but was unsuccessful since the yttrium signal was so weak that no unique solution for the EXAFS could be found. However, the information from this attempt was useful in putting upper bounds on the contributions of the Fe-Y pairs to the iron EXAFS.

Since no good standard materials exist from which to extract empirical phase-shift and backscattering functions, these functions were approximated by using the calcula-

tions of Teo and Lee.[10] As a check, these calculations were used to fit the Fe EXAFS of Fe_2Y, whose structure is well known.

The results of fitting the Fe EXAFS data for the amorphous alloy are given in Table I in which $R=r_0+3\sigma$ (average distance). The Fe-to-Y near-neighbor ratio has been corrected based on the analysis of the known Fe_2Y. If, as the XANES spectra indicate, each iron atoms has 12 near neighbors, the ratio N_{Fe}/N_Y dictates that the average iron atom is surrounded by ten iron and two yttrium atoms. The reconstructed pair distribution functions using Eq. (1) shown in Fig. 4.

B. Magnetic measurements

As a test for spin-glass behavior, the sample was mounted and cooled at 5 K in zero field and the suscepti-
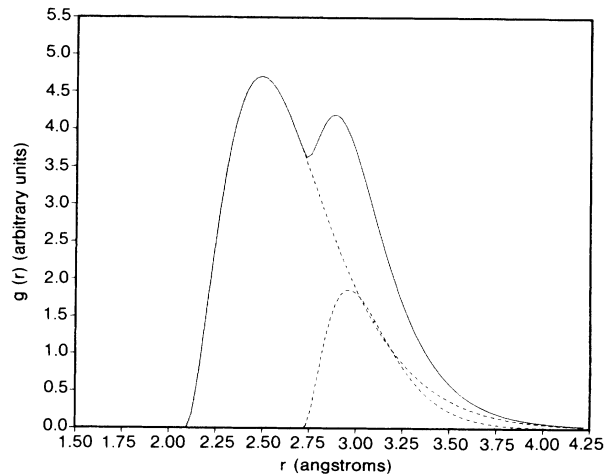

FIG. 4. Reconstructed near-neighbor distribution from Eq. (1). Solid line is the total distribution, and the dashed lines are the partial Fe-Fe and Fe-Y distributions.
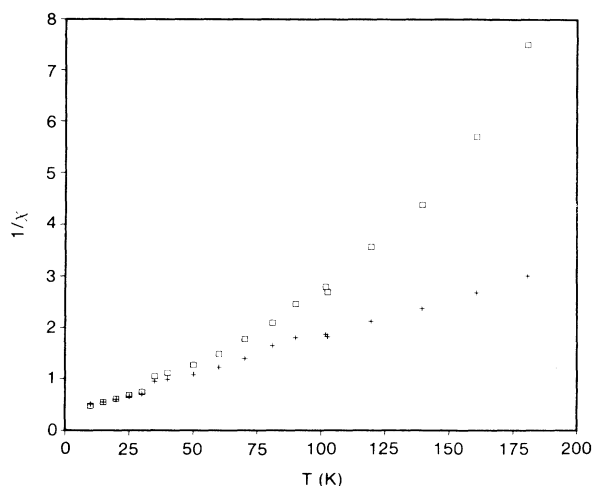
FIG. 5. Inverse susceptibility for film plus substrates (squares) and film (crosses).

bility was subsequently measured in a 0.3-kOe field as the temperature increased. The susceptibility was a smooth, monotonically decreasing function as the temperature increased: there was no evidence of either (i) a peak or (ii) a nonmonotonic change in the derivative of susceptibility with respect to temperature—an indication of a peak that has been broadened by the applied field. In later measurements at fixed low temperatures, the applied field was cycled from near zero to 5 kOe and back to near zero: there was no evidence of irreversible behavior. From these features we conclude that the sample is not a spin glass. Magnetization-versus-field sequences at low temperatures were reproducible with no evidence of hysteresis and exhibited a weak but clear curvature; this curvature decreased with increasing temperature. More details on this curvature are provided below in Sec. V. The major result of the magnetic studies is given in Fig. 5, where susceptibility data for the amorphous film plus substrate and for just the amorphous film are plotted as a function of temperature. These data were taken with an applied field of 5 kOe. The data for the $Fe_{0.30}Y_{0.70}$ film are consistent with a Curie-Weiss law. When the arbitrary units are converted into absolute units, the slope for the data indicate a moment of $4\mu_B$ per molar unit or a moment of $6.9\mu_B$ per Fe atom assuming that the Y atoms have no moment. Either value is too large for a single Fe atom.

C. EELS spectra

The electron-energy-loss spectra shown in Fig. 6 compare the L_{III}, L_{II}-edge spectra of pure iron and that of the $Fe_{0.30}Y_{0.70}$ amorphous alloy. There is a decrease in

TABLE I. Results of fitting the Fe EXAFS data for amorphous alloys.

	r_0	σ	$\overline{R}$	N_{Fe}/N_Y
Fe-Fe	2.09	0.23	2.78	5/1
Fe-Y	2.77	0.10	3.07	
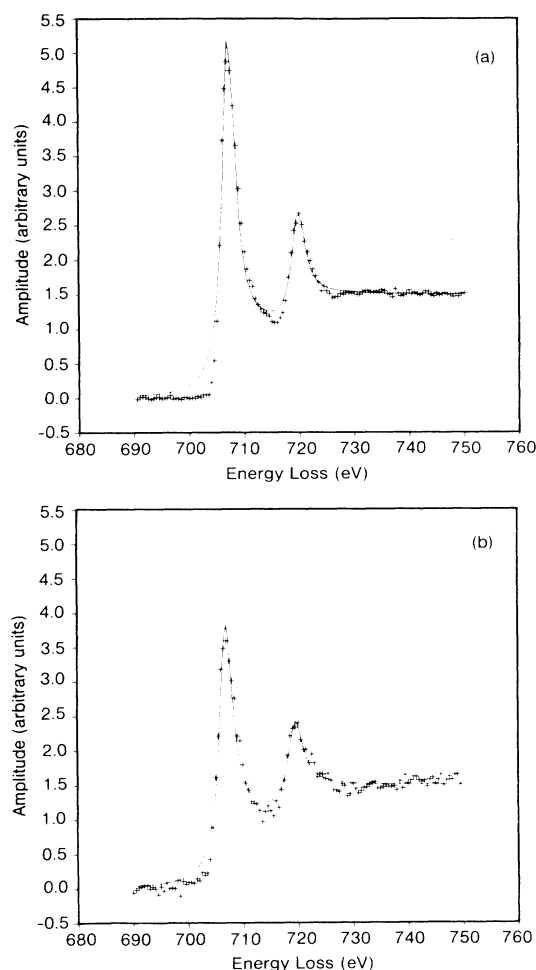
FIG. 6. Fe L_{III},L_{II} spectra for (a) pure iron and (b) amorphous $Fe_{0.30}Y_{0.70}$. Crosses represent experimental data and solid lines show best fit described in text.

the overall amplitude of the peaks in the spectrum of the amorphous alloy relative to that of the pure metal, and it can also be seen that the ratio of the amplitudes of the L_{III} and L_{II} peaks changes. These observations can be further quantified using analysis methods described in Ref. 5, in which the peaks are approximated by Lorentzians and the steplike continuum backgrounds are approximated by arctangent functions.[11] Table II gives the results of this analysis for the energy-loss spectra.

IV. DISCUSSION

It is apparent from the Fe-to-Y ratio about the iron atoms in the amorphous alloy that the alloy cannot be described as a random packing of hard spheres. For

TABLE II. $A(L_{III})$ and $A(L_{II})$ are the white-line peak areas normalized to the total number of iron atoms in the electron beam. See Ref. 5.

	$A(L_{III})$	$A(L_{II})$	$A(L_{III})/A(L_{II})$
Fe	57.2	17.0	3.4
$Fe_{0.30}Y_{0.70}$	47.4	20.5	2.3

random close-packed systems, Chappert et al.[12] point out that the probability distribution of N yttrium atoms about iron in $Fe_x Y_{1-x}$ can be written

$$P(N) = \frac{12!(1-x)^N x^{12-N}}{N!(12-N)!} . \tag{4}$$

This distribution for $x = 0.3$ in Fig. 7 shows that the probability of finding ten iron atoms and two yttrium atoms around iron is vanishingly small in a truly random amorphous alloy. We are forced to conclude that there is significant short-range ordering in the form of iron cluster formation.

From the EXAFS data it is possible to construct a model for the iron clusters. If we assume a spherical cluster, the 10:2 Fe:Y ratio dictates that the average cluster would have a diameter of about eight atoms and would contain about 260 atoms. If such clusters were distributed throughout a highly disordered yttrium matrix they would be difficult, if not impossible, to image via transmission electron microscopy in a 300-Å sample. Consequently, we can make no claims about the actual shape or size distributions of the clusters.

Given the pair distribution function determined by the EXAFS we can begin to make a phenomenological description of how disorder can affect the magnetic properties of a material within a simple mean field model. In a direct exchange crystalline system, the magnetization depends on the number of interacting spins and an interatomic-distance-dependent exchange parameter J_{ij}. For a given lattice, this coupling can be expressed as a convolution of some function $J(R)$ and a sum of δ functions $\delta(R - R_j)$ representing a pair distribution function. In an amorphous alloy, though, it is necessary to replace these discrete interatomic distances with a continuous distribution of magnetic atoms; for direct exchange, we need consider only nearest neighbors and thus it is appropriate to use the partial near-neighbor distribution function, $J(R)$, obtained from an EXAFS experiment. In amorphous materials, the Hamiltonian describing magnetic interactions must be expressed in terms of a convolution of both $J(R)$ and $g(R)$.[1(b)]

Two features of the magnetic data require clarification prior to any discussion of the detailed results. First, no corrections for demagnetization effects have been applied. A typical portion of the magnetic sample was approxi-

FIG. 7. Probability histogram of N yttrium near neighbors about Fe in $Fe_{0.30}Y_{0.70}$ from Eq. (4).

mately 3 mm square and 0.0005 mm thick. Mounting such portions parallel to the magnetic field meant the demagnetizing factor was less than 10^{-3} and thereby justified the omission of corrections.[13] Second, there is an apparent discontinuity in the susceptibility data between 30 and 35 K. This continuity was reproducible. However, this temperature range is the region where the net paramagnetism contribution from the film plus substrate was just canceled by the diamagnetic contribution from the Kel-F holder. Thus, the magnetometer effectively had "no sample"; past experience indicates unusual and unphysical "results" can be observed under this condition. Since the susceptibility of the actual sample continues to increase smoothly at lower temperatures, we have treated this discontinuity as an artifact and have fitted the entire data set to a single Curie-Weiss equation.

The magnetic properties of amorphous $Fe_x Y_{1-x}$ have been the subject of several studies and, in particular, Coey et al.[14] reported a detailed investigation of the magnetic properties for $0.32 \leq x \leq 0.88$. Their data indicated applied fields of 100 kOe or greater were required to estimate saturation behavior reliably. From such saturation data they found that the magnetic moment per Fe atom, μ_{Fe}, increased linearly with x from $0.2 \leq x \leq 0.7$. In general, their data indicate systematic changes in magnetic properties as x increases. They report spin-glass behavior, asperomagnetic spin structures, and evidence of band metamagnetism. Coey et al. concluded that their study provided evidence of competing ferromagnetic and antiferromagnetic interactions.

Our magnetic results are generally consistent with those of Coey et al. We find no evidence of spin-glass behavior down to 6 K in our $x = 0.3$ sample; they found no evidence of spin-glass behavior in an $x = 0.32$ sample. We find a weak but definite curvature in M versus H at lower temperature. This is an expected precursor to the saturation behavior Coey et al. found at fields 10-40 times our applied field. The absolute value of susceptibility for our sample is comparable (i.e., within a factor of 2) to the absolute value reported by Coey et al. for an $x = 0.32$ sample.

The agreement between the magnetic results is even more striking when the $6.9\mu_B$ per Fe atom obtained from our susceptibility data is considered. This value is more than 3 times the value obtained for pure iron and thus is physically unreasonable as it stands. However, the EXAFS data indicate that the Fe atoms are not randomly distributed but are clustered. For susceptibility data the moment of a cluster can increase with the number of atoms in the cluster, but there is a related decrease in the number of contributing clusters. Assuming that only Fe atoms have moments, the net result of these related changes is a susceptibility moment of $\sqrt{N}\mu_{Fe}$, where N is the number of Fe atoms in the cluster. The EXAFS data indicate the clusters involve 260 atoms and this corresponds to μ_{Fe} of $0.42\mu_B$. This value is in reasonable agreement with the value of $0.36\mu_B$ reported by Coey et al. for an $x = 0.32$ sample. Their result was obtained from saturation data.

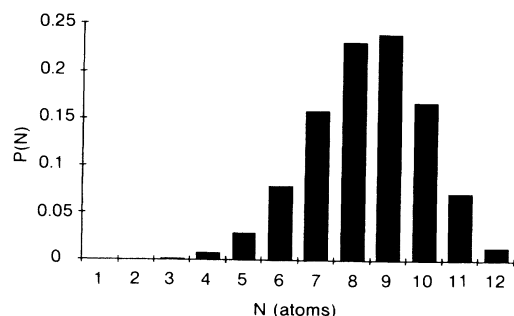The L-edge EELS data can be interpreted as further evidence of the reduced magnetic moment in the amorphous

alloy. Since the overwhelming contributions to the L_{III}, L_{II} peak intensities comes from p-d transitions,[15] an overall decrease in the peak intensities could be interpreted as a decrease in the number of holes in the d band. In addition, the decrease in the L_{III}/L_{II} amplitude ratio can correspond to an interband electron transfer between the $d_{5/2}$ and $d_{3/2}$ subbands,[5] resulting in decreased spin pairing for atoms with d shells that are more than half-filled.

There is a conceptual approach which has all the features of reduced moments, competing ferromagnetic and antiferromagnetic interaction, and an expected field dependence for magnetization. The presence of Fe atom clusters can be viewed as stabilizing one form of Fe in another matrix and the twelve-fold coordination of atoms suggests thinking of close-packed arrangements similar to face-centered cubic (fcc). fcc iron is antiferromagnetic with a small magnetic moment. The traditional Slater-Pauling curve explains this behavior on the basis of an interaction that changes from ferromagnetic to antiferromagnetic as the separation of the nearest neighbors increases. bcc Fe, with a lattice parameter of 2.8664 Å,[16] has a nearest-neighbor distance of 2.482 Å and is ferromagnetic, while fcc Fe, with a lattice parameter of 3.6468 Å,[16] has a nearest-neighbor distance of 2.5791 Å and is antiferromagnetic. Crystalline fcc Fe is a single entry on the Slater-Pauling curve but the Fe clusters in our $Fe_{0.30}Y_{0.70}$ sample would correspond to a distribution of distances. This distribution samples both the ferromagnetic and antiferromagnetic interactions.

The recent local spin-density-functional calculation by Kubler[17] provides an alternative to the traditional Slater-Pauling curve. Kubler's calculations predict that an expansion of the fcc Fe lattice causes the antiferromagnetic state and the ferromagnetic state to become degenerate. For each state the value of μ_{Fe} is a function of lattice parameter. Assuming that the antiferromagnetic-ferromagnetic transformation is due only to short-range, rather than long-range, order, these results indicate that the Fe cluster could be viewed as a stabilized close-packed structure with a range of nearest-neighbor distances that could sample the a distribution of magnetic interactions; the average iron atom would experience an effective field due to spatially varying moments and a distance-dependent exchange function $J(R)$ that could change sign within the width of the near-neighbor distance distribution.

We conclude, then, that in the study of amorphous alloys it is an oversimplification to assume that the local ordering can be described as a dense random packing of hard spheres. The majority of the EXAFS studies performed to date[1-4] have repeatedly demonstrated that, since amorphous materials are metastable in a thermodynamic sense, the presence or absence of clustering or other forms of compositional short-range order cannot be ignored. Truly random arrangements of atoms can most certainly exist, depending on preparation conditions, cooling rates, or thermal histories, but it seems that a random packing of hard spheres must be treated as a special, rather than a general, case. This fact alone accounts undoubtedly for the often contradictory results obtained on different amorphous samples of the same composition prepared in different laboratories under different conditions.

ACKNOWLEDGMENTS

*Permanent address: Physics Department, Illinois Institue of Technology, 3100 S. Dearborn, Chicago, IL 60616.

[1]See, for example, (a) K. Moorjani and J. M. D. Coey, in *Metallic Glasses*, edited by S. P. Wolsky (Elsevier, New York, 1984), and references cited therein; (b) Takahito Kaneyoshi, in *Amorphous Magnetism* (Chemical Rubber Co. Press, Inc., Boca Raton, FL, 1984), and references cited therein; *Amorphous Metallic Alloys*, edited by F. E. Luborsky (Butterworths, London, 1983), and references cited therein.

[2]T. I. Morrison, Phys. Lett. **112A**, 85 (1985).

[3]A. Sadoc, D. Raoux, P. Lagarde, and A. Fontaine, J. Non-Cryst. Solids **50**, 331 (1982).

[4]A. Sadoc and Y. Calvayrac, J. Non-Cryst. Solids (to be published).

[5]T. I. Morrison, M. B. Brodsky, L. R. Sill, and N. J. Zaluzec, Phys. Rev. B **32**, 3107 (1985).

[6]T. I. Morrison, L. E. Iton, G. K. Shenoy, G. D. Stucky, and S. L. Suib, J. Chem. Phys. **75**, 4086 (1981).

[7]B. Bunker (private communication). See also R. Zeller, G. Stegman, and B. Lengeler (unpublished).

[8]P. Eisenberger and G. S. Brown, Solid State Commun. **29**, 481 (1979).

[9]E. D. Crozier and A. J. Seary, Can. J. Phys. **58**, 1388 (1980).

[10]B.-K. Teo and P. A. Lee, J. Am. Chem. Soc. **101**, 2815 (1979).

[11]J. A. Horsely, J. Chem. Phys. **76**, 1451 (1982).

[12]J. Chappert, R. Arrese-Boggiano, and J. M. D. Coey, J. Mag. Magn. Mater. **7**, 175 (1978).

[13]Richard M. Bozorth, *Ferromagnetism* (Van Nostrand, New York, 1951), pp. 845 ff.

[14]J. M. D. Coey, D. Givord, A. Lienard, and J. P. Rebouillat, J. Phys. F **11**, 2707 (1981).

[15]L. F. Matheiss and R. E. Dietz, Phys. Rev. B **22**, 1663 (1980).

[16]W. B. Pearson, in *Handbook of Lattice Spacings and Structures of Metals* (Pergamon, New York, 1967), Vol. 2.

[17]J. Kubler, Phys. Lett. **81A**, 81 (1981).